ONLINE SUPPLEMENTAL MATERIAL –

LEGENDS TO 9 SUPPL. VIDEOS AND 7 SUPPL. FIGURES

Supplementary Video 1. FMT-CT analysis of pulmonary MMP activity in three dimensions. Three-dimensional virtual rendering shows MMP activity in inflamed lung. The animation is a representative reconstruction and fusion of the FMT and CT recordings.

Supplementary Video 2. FMT analysis of pulmonary MMP activity in a control mouse. FMT acquisition data set through ~1cm show a coronal image reconstruction of a region of interest encompassing the lung of a control (unchallenged) mouse.

Supplementary Video 3. FMT analysis of pulmonary MMP activity in a mouse with moderate airway inflammation. FMT acquisition data set through ~1cm show a coronal image reconstruction of a region of interest encompassing the lung of a mouse with moderate airway inflammation.

Supplementary Video 4. FMT analysis of pulmonary MMP activity in a mouse with potent airway inflammation. FMT acquisition data set through ~1cm show a coronal image reconstruction of a region of interest encompassing the lung of a mouse with potent airway inflammation.

Supplementary Video 5. Video-assisted microcatheter NIRF bronchoscopy for real-time visualization of MMP activity in mouse conducting airways. An imaging microcatheter consisting of a 300 μm outer diameter fiber connected to a collection unit is atraumatically advanced through third order branches within mouse bronchi to report on MMP activity in vivo.

Supplementary Video 6. NIRF bronchoscopic analysis of MMP activity in a control (unchallenged) mouse. The procedure is detailed in Supplementary Figure 5.

Supplementary Video 7. NIRF bronchoscopic analysis of MMP activity in a mouse with potent airway inflammation. The procedure is detailed in Supplementary Figure 5.

Supplementary Video 8. NIRF bronchoscopic analysis of MMP activity in a mouse treated with the glucocorticoid dexamethasone ('D'). The detailed is explained in Supplementary Figure 5.

Supplementary Video 9. NIRF bronchoscopic analysis of MMP activity in a mouse treated with a novel self-activating viridin prodrug ('S'). The detailed is explained in Supplementary Figure 5.

Supplementary Figure 1. Generation of moderate or potent airway inflammation using two different protocols. (A) Protocols to generate moderate ('×1', i.e. animals sensitized once with OVA/Alum) or potent ('×2', i.e. animals sensitized twice with OVA/Alum) allergic airway inflammation. **(B)** Characterization of cell infiltrates in bronchoalveolar lavage (BAL) fluids of mice with moderate or potent allergic inflammation. Unchallenged mice served as controls. **(C)** IL-5 levels in BAL fluids of the same mice. *$p<0.05$.

Supplementary Figure 2. FMT analysis of MMP activity in lungs. (A) Schematic representation of the FMT set up. **(B)** Sagittal, axial, and coronal stacks with defined regions of interest (ROI) around the lung to determine ultimately the volume of interest (VOI), and **(C)** further confirmed by FMT-CT fusion imaging. **(D)** Three-dimensional tomographic reconstruction of optical signal from the lung with X, Y and Z projections. **(E)** Z stacks of tomographic data sets (through ~ 1cm of lung tissue) from representative mice with no, moderate or potent allergic airway inflammation.

Supplementary Figure 3. Heartbeat and respiratory monitoring readouts during isoflurane anesthesia. (**A**) Electrocardiogram of a mouse under the effects of the gas anesthetic isoflurane. (**B**) Respiratory monitoring readout during isoflurane anesthesia shows that inspiration comprises only 10-20% of the respiratory cycle (downward slope). During inspiration, the chest wall moves out and the diaphragm moves caudally by ~1-2mm. Since FMT imaging is performed continually, the acquisition is heavily weighted towards the expiratory/inactive state. However there may be some degree of partial

volume effects or motion-induced artifacts. This movement is in the range of the spatial resolution of the FMT system.

Supplementary Figure 4. FMT analysis of MMP and cathepsin activities in lungs. MMP (green) and cathepsin (pink) activity co-registered by FMT in whole lungs of mice with no (unchallenged), moderate (sensitized once with OVA/Alum) or potent (sensitized twice with OVA/Alum) airway inflammation (* $p<0.05$).

Supplementary Figure 5. MMP activity in MMP-12–deficient mice. (A-B) Ex vivo FRI analysis of MMP activity in excised lungs of wild type and MMP-12–deficient mice; **$p<0.01$. **(C)** In vitro activity of the pan-MMP sensor against various MMPs analyzed individually.

Supplementary Figure 6. In vivo detection of MMP activity in LPS-mediated pulmonary inflammation. (A) Characterization of cell infiltrates in bronchoalveolar lavage (BAL) fluids of mice with LPS-mediated pulmonary inflammation or with OVA-mediated allergic airway inflammation. LPS-treated mice received a ~15µg single dose of LPS and were analyzed at 6h (pink), 18h (red), and 24h (dark red) post LPS administration. OVA-treated mice were sensitized twice (X2) with OVA/Alum and then challenged 4 times with OVA (blue), and analyzed 24h after the last OVA challenge. Control mice received PBS instead of LPS (gray). (B) H&E staining of cells obtained from BAL fluids of PBS-control mice, LPS-treated mice (24h), or OVA-treated mice. (C)

Quantification of cell populations from single cell suspensions of digested lungs. (D) FMT measurement of in vivo MMP activity in the lungs. (E) Flow cytometric analysis of single-cell suspensions from lungs. At least two independent experiments were performed with n=3-5 animals per experiment and per group. Data are shown as mean ± SEM.

Supplementary Figure 7. Therapeutic efficacy of dexamethasone and self-activating viridin prodrug. (A) Ex vivo analysis of BAL fluids indicates that administration of D (dexamethasone) or S (self-activating viridin prodrug) decreases the number of lung eosinophils. Control mice received a non-activating drug (N) that does not release viridin, or the drug vehicle dextran alone (V). **(B)** IL-5 levels in BAL fluids of the same mice. *$p<0.05$.

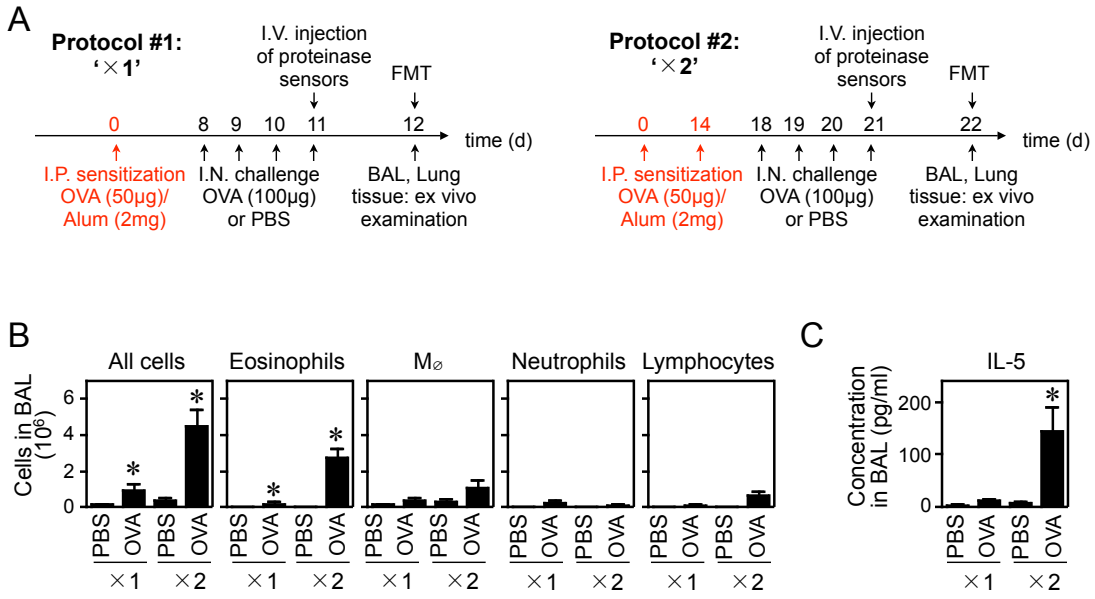

Supplementary Figure 1. Generation of moderate or potent airway inflammation using two different protocols. (A) Protocols to generate moderate ('×1', i.e. animals sensitized once with OVA/Alum) or potent ('×2', i.e. animals sensitized twice with OVA/Alum) allergic airway inflammation. **(B)** Characterization of cell infiltrates in bronchoalveolar lavage (BAL) fluids of mice with moderate or potent allergic inflammation. Unchallenged mice served as controls. **(C)** IL-5 levels in BAL fluids of the same mice. *p<0.05.

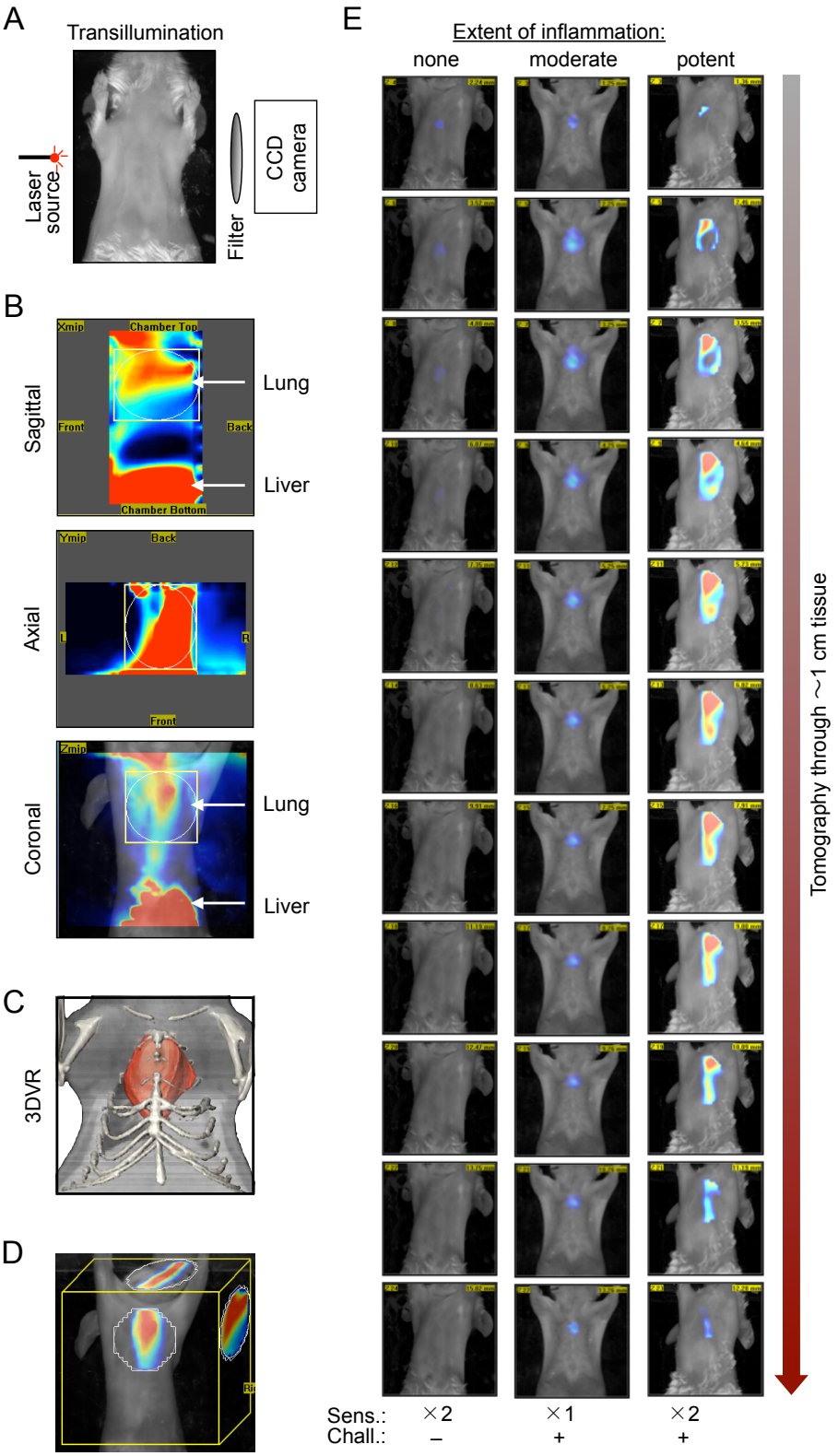

Supplementary Figure 2. FMT analysis of MMP activity in lungs. (A) Schematic representation of the FMT set up. **(B)** Sagittal, axial, and coronal stacks with defined regions of interest (ROI) around the lung to determine ultimately the volume of interest (VOI), and **(C)** further confirmed by FMT-CT fusion imaging. **(D)** Three-dimensional tomographic reconstruction of optical signal from the lung with X, Y and Z projections. **(E)** Z stacks of tomographic data sets (through ~ 1cm of lung tissue) from representative mice with no, moderate or potent allergic airway inflammation.

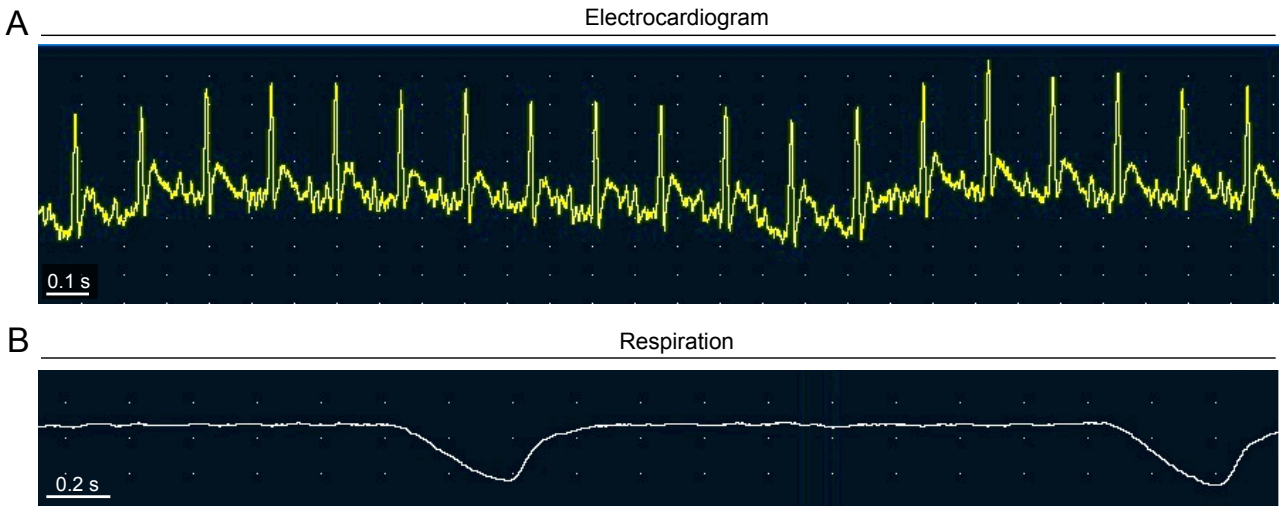

Supplementary Figure 3. Heartbeat and respiratory monitoring readouts during isoflurane anesthesia. (A) Electrocardiogram of a mouse under the effects of the gas anesthetic isoflurane. **(B)** Respiratory monitoring readout during isoflurane anesthesia shows that inspiration comprises only 10-20% of the respiratory cycle (downward slope). During inspiration, the chest wall moves out and the diaphragm moves caudally by ~1-2mm. Since FMT imaging is performed continually, the acquisition is heavily weighted towards the expiratory/inactive state. However there may be some degree of partial volume effects or motion-induced artifacts. This movement is in the range of the spatial resolution of the FMT system.

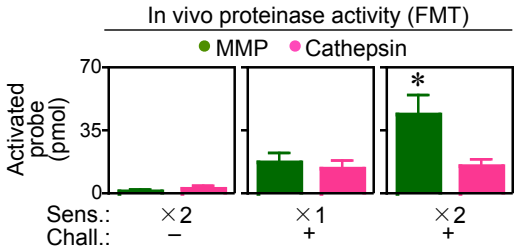

Supplementary Figure 4. FMT analysis of MMP and cathepsin activities in lungs. MMP (green) and cathepsin (pink) activity co-registered by FMT in whole lungs of mice with no (unchallenged), moderate (sensitized once with OVA/Alum) or potent (sensitized twice with OVA/Alum) airway inflammation (* $p<0.05$).

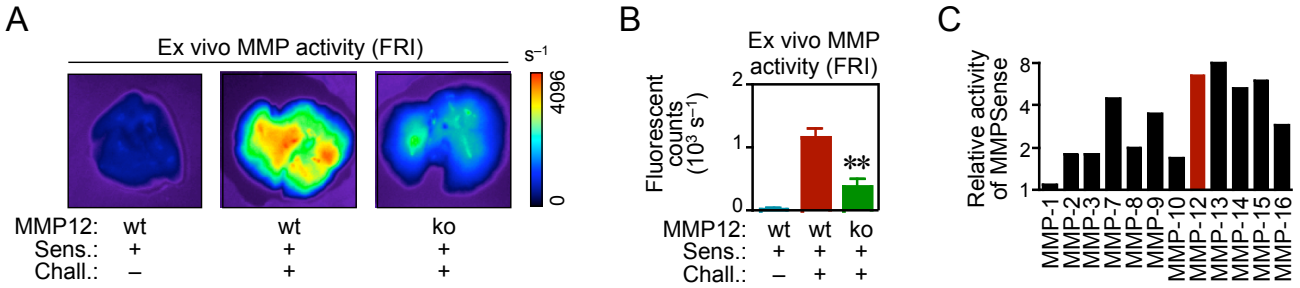

Supplementary Figure 5. MMP activity in MMP-12–deficient mice. (A-B) Ex vivo FRI analysis of MMP activity in excised lungs of wild type and MMP-12–deficient mice; **p<0.01. **(C)** In vitro activity of the pan-MMP sensor against various MMPs analyzed individually.

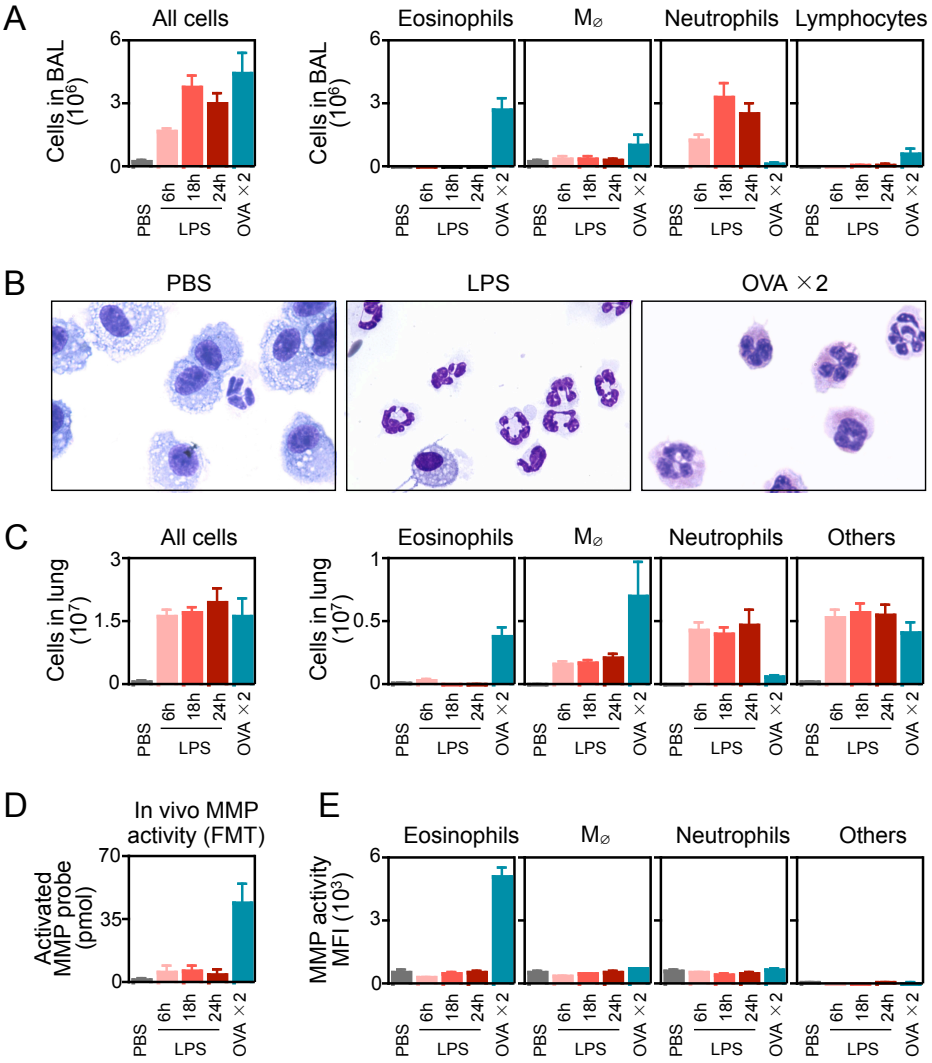

Supplementary Figure 6. In vivo detection of MMP activity in LPS-mediated pulmonary inflammation. **(A)** Characterization of cell infiltrates in bronchoalveolar lavage (BAL) fluids of mice with LPS-mediated pulmonary inflammation or with OVA-mediated allergic airway inflammation. LPS-treated mice received a ~15µg single dose of LPS and were analyzed at 6h (pink), 18h (red), and 24h (dark red) post LPS administration. OVA-treated mice were sensitized twice (X2) with OVA/Alum and then challenged 4 times with OVA (blue), and analyzed 24h after the last OVA challenge. Control mice received PBS instead of LPS (gray). **(B)** H&E staining of cells obtained from BAL fluids of PBS-control mice, LPS-treated mice (24h), or OVA-treated mice. **(C)** Quantification of cell populations from single cell suspensions of digested lungs. **(D)** FMT measurement of in vivo MMP activity in the lungs. **(E)** Flow cytometric analysis of single-cell suspensions from lungs. At least two independent experiments were performed with n=3-5 animals per experiment and per group. Data are shown as mean ± SEM.

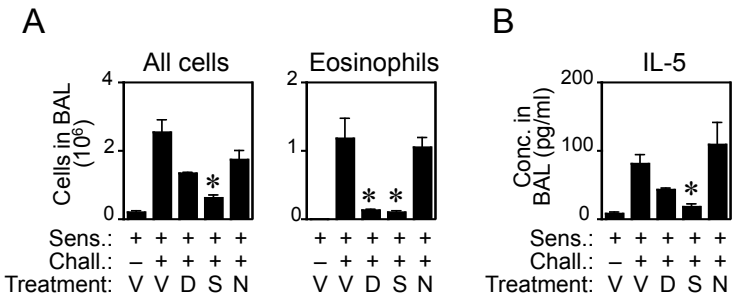

Supplementary Figure 7. Therapeutic efficacy of dexamethasone and self-activating viridin prodrug. (A) Ex vivo analysis of BAL fluids indicates that administration of D (dexamethasone) or S (self-activating viridin prodrug) decreases the number of lung eosinophils. Control mice received a non-activating drug (N) that does not release viridin, or the drug vehicle dextran alone (V). **(B)** IL-5 levels in BAL fluids of the same mice. *p<0.05.